Catalysis Science & Technology

ROYAL SOCIETY OF CHEMISTRY

COMMUNICATION

View Article Online
View Journal | View Issue

Cite this: *Catal. Sci. Technol.*, 2023, 13, 2922

Received 12th April 2023,
Accepted 26th April 2023

DOI: 10.1039/d3cy00494e

rsc.li/catalysis

Unravelling the mechanism of CO_2 activation over low-loaded $Cu/CeO_2(111)$ catalysts using *operando* and transient spectroscopies†

Marc Ziemba and Christian Hess *

Using *operando* Raman and UV-vis spectroscopy as well as transient IR spectroscopy, low-loaded $Cu/CeO_2(111)$ catalysts were investigated with respect to their redox behavior and the importance of adsorbates for the reverse water–gas shift (rWGS) reaction. Here it is shown that of two possible mechanisms the redox mechanism is predominant over an associative one.

Cu/CeO_2 catalysts show excellent properties in redox reactions, such as CO oxidation,[1] (reverse) water–gas shift ((r)WGS) reaction[2–4] or methanol synthesis,[5] and are less expensive and environmentally demanding than, for example, Au/CeO_2 or Pt/CeO_2.[6] Besides, they exhibit additional positive features, as, unlike gold, copper does not tend to agglomerate at the surface under WGS reaction conditions.[7,8] The reverse WGS reaction is of great interest in the context of CO_2 utilization to counteract global warming (CO_2 reacting with regeneratively produced H_2 to give CO). Previous studies have already shown the potential of high-loaded Cu/CeO_2 (15 wt% Cu) for the rWGS reaction.[9] In another study with 5 wt% Cu/CeO_2, the facet dependence was addressed and ceria rods were identified as more active than nanospheres, probably due to higher bidentate carbonate and formate coverages.[4] In contrast, studies with very low Cu loadings (≤0.5 wt%) are rare, although such loadings may be of particular interest for single-atom catalysts, which have already shown excellent properties in WGS.[10] In studies performed to this end, our ≤0.5 wt% Cu/CeO_2 catalysts revealed high WGS activity.[7]

In the literature, typically either redox or associative mechanisms are proposed in the context of (r)WGS reactions. To differentiate accurately between these mechanisms, it is important to apply a variety of methods to identify, on one hand, the redox dynamics of the support and, on the other, the direct involvement of adsorbates in the reaction. To this end, our previous studies have shown that a combination of *operando* Raman and UV-vis spectroscopy allows the oxygen dynamics to be monitored, whereas transient DRIFT (diffuse reflectance infrared Fourier transform) spectroscopy can identify possible intermediates.[7,11] Besides, the copper state should be taken into account, but *operando* spectroscopic characterization at low loadings (≤0.5 wt% Cu) is challenging. In principle, quantitative statements can be made based on *operando* UV-vis spectroscopy, while the information provided by X-ray photoelectron spectroscopy (XPS) is limited but may be used to support these statements. To probe the various aspects of low-loaded Cu/CeO_2 catalysts and to gain insight into the rWGS reaction mechanism, we have combined the previously mentioned spectroscopic methods and compared our results with those previously obtained for Au/CeO_2 catalysts,[11] thus highlighting the role of the supported metal.

The Cu/CeO_2 sheets and polyhedra were prepared as described previously[7] and the Cu loading was determined to be 0.42 and 0.43 wt%, respectively, using inductively coupled plasma optical emission spectrometry (ICP-OES). The specific surface areas of the catalysts were determined by N_2 adsorption (BET) in previous studies and are 36 m^2 g^{-1} for

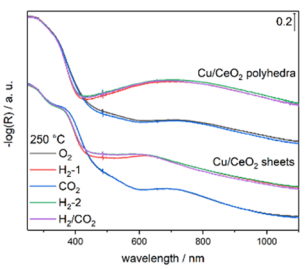

Fig. 1 *In situ*/*operando* UV-vis reflectance spectra of Cu/CeO_2 sheets (bottom) and polyhedra (top) at 250 °C for the indicated gas atmospheres.

Eduard Zintl Institute of Inorganic and Physical Chemistry, Technical University of Darmstadt, Alarich-Weiss-Str. 8, 64287 Darmstadt, Germany.
E-mail: christian.hess@tu-darmstadt.de

† Electronic supplementary information (ESI) available: Additional characterization data and experimental details. See DOI: https://doi.org/10.1039/d3cy00494e

the polyhedra and 57 m^2 g^{-1} for the sheets. TEM images are shown in Fig. 1 from our previous study.[11] Based on our previous study[7] and studies by Yao and co-workers for a sample with a loading of 1.9 wt% Cu,[12] for which a full dispersion was observed by N_2O–CO temperature-programmed desorption (TPD), we can expect a similar dispersion for our samples, as in both syntheses the deposition–precipitation method was used. While both samples exhibit a CeO_2(111)-terminated surface, the sheets show additional stepped CeO_2(111) sites.[11]

For the mechanistic studies, both samples were characterized using *operando* Raman (λ_{ex} = 532 nm) and *operando* UV-vis spectroscopy at 250 °C under different gas atmospheres, *i.e.*, O_2 (10 vol%), H_2 (4 vol%), CO_2 (2 vol%), or H_2/CO_2 (4/2 vol%), balanced by Ar at a total flow rate of 100 ml min^{-1} (for experimental methods see ESI†). Using quantitative gas-phase IR analysis of the exhaust, the CO_2 conversions were determined as 6.6 % for the sheets and 3.0 % for the polyhedra, at a CO selectivity of 100 %. In comparison to the corresponding Au/CeO_2 catalysts,[11] which show a similar activity for sheets and polyhedra, Cu/sheets are more than twice as active as Cu/polyhedra and slightly more active than the gold catalysts. Besides, Cu/polyhedra show a strong decrease in activity with time (see Fig. S1†), indicating a change of the catalyst during the reaction, which will be discussed later based on *operando* spectroscopic results. For this reason, the aforementioned activities were recorded after approximately one hour within the second reaction phase to minimize possible deactivation processes that may occur at the beginning and to reach a steady state.

We start with the UV-vis results. Fig. 1 depicts *operando* spectra of the two Cu/CeO_2 catalysts, in comparison to *in situ* spectra recorded under oxidizing and reducing gas atmospheres. Thereby, the visible range is of particular interest, where Ce^{4+}–Ce^{3+} charge transfer transitions (broad),[13] absorption bands of Cu^+ and/or $[Cu_2O]^{2+}$ species (400–470 nm), and d–d Cu^{2+} transitions (600–850 nm) are located.[14–16] In addition, metallic copper may be detectable *via* surface plasmons (520–580 nm),[17,18] but these are expected to play a minor role due to high dispersion.

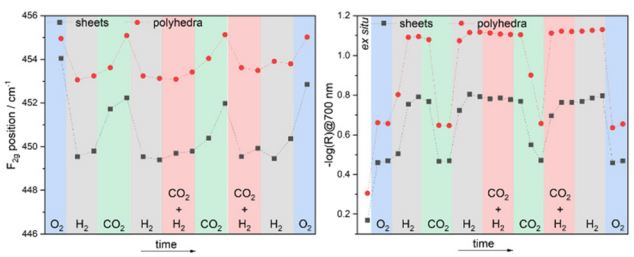

Fig. 2 *In situ*/*operando* Raman (left) and UV-vis (right) results for Cu/CeO_2 catalysts recorded during the indicated gas exposures at 250 °C and at a total flow rate of 100 ml min^{-1}. UV-vis spectra were recorded before and after the Raman spectra. The gas exposure was always about one hour, with the exception of O_2, which was only about 30 min. Raman spectra were recorded at 532 nm laser excitation.

Both samples are characterized by strong absorption in the visible range, in contrast to the bare samples (see Fig. 2), which show only a slight broad increase in the visible range after the reaction phase and the second H_2 phase, which is due to ceria reduction. Thus, the stronger absorption of the Cu/CeO_2 samples must be caused by the presence of copper. Concerning ceria reduction, the stronger broad increase for the Cu/CeO_2 samples under reducing atmospheres (H_2 and H_2/CO_2) can be explained by the positive influence of copper on the reduction behavior.[19] When the Cu/CeO_2 samples are exposed to O_2 and CO_2, mainly contributions from Cu^+ (400–470 nm) and Cu^{2+} (600–850 nm) are observed, whereby the absorptions are sharper for the sheets, suggesting a greater proportion of cationic copper species. The presence of Cu^{2+} species is supported by quasi *in situ* XP spectra (see Fig. S3†), which reveal shake up signals typical for Cu^{2+}. Under reductive conditions, the Cu^{2+} absorption shifts to lower wavelengths. According to previous studies, such a red-shift may be attributed to a change in the Cu^{2+} environment from more or less tetragonally distorted O_h symmetry to bulk CuO.[20] For the polyhedra, rather a broad increase is detected, which is attributed to the redox behavior of ceria. Summarizing the UV-vis results, for the sheets, there are more cationic copper species on the surface and the environment of the Cu^{2+} species is subject to changes in the presence of H_2, which could represent possible reasons for the higher activity of the sheets.

To gain more detailed insight into the reduction behavior of the support, the position of the F_{2g} Raman band was used as an indicator for the reducibility, where the F_{2g} band is the first order allowed Raman band in crystalline CeO_2. Besides the F_{2g} band the absorption increase at 700 nm from the UV-vis spectra. This value was selected exemplarily for the 500–800 nm range, *i.e.*, other wavelengths in this region show the same trend. However, it should be noted that this region also overlaps with Cu^{2+}. Both signals (Raman, UV-vis) have previously been shown to be excellent indicators of ceria reducibility, also under *operando* conditions.[7,8,11,21] Briefly, an F_{2g} red-shift represents ceria reduction and a blue-shift, ceria oxidation, which can be explained by the larger ionic radius of Ce^{3+} (ref. 22) leading to an expansion of the crystal lattice. This thus directly affects the lattice parameter, which in turn influences the F_{2g} position. The use of the absorption in the visible range as an indicator is based on the broad signal from the Ce^{4+}–Ce^{3+} charge transfer transitions, which shows an increase if, as a result of support reduction, more Ce^{3+} is present. Applying this approach to the Cu/CeO_2 catalysts, Fig. 2 depicts the F_{2g} positions from the Raman spectra (left) and the absorption at 700 nm from the UV-vis spectra (right) for the different gas atmospheres. As can be seen from the F_{2g} band position of the sheets (black) and the polyhedra (red), both supports are reduced in H_2 and under reaction conditions. Upon subsequent CO_2 treatment, the F_{2g} band shifts to the blue again, showing that CO_2 alone can oxidize the support under the release of CO (as shown by gas-phase IR spectra, see Fig. S1†). For both atmospheres (H_2,

H_2/CO_2), a similar extent of reduction is observed, which shows that in the case of a pure redox mechanism, the reduction predominates over the oxidation or takes place significantly faster. The comparison between the sheets and the polyhedra also shows differences in the absolute values of the F_{2g} shifts. In fact, when switching from the first H_2 to the CO_2 phase, blue-shifts of 2.7 cm^{-1} and 2.0 cm^{-1} are detected for the sheets and polyhedra, respectively, implying that the sheets are slightly more reduced than the polyhedra. While the UV-vis results in the right panel of Fig. 2 show an overall trend similar to that of the Raman data, upon closer inspection, differences can be seen, *i.e.*, the absolute change in absorbance on switching from H_2 to CO_2 or *vice versa* is larger for the polyhedra. This was not the case for our Au/CeO_2 catalysts, although polyhedra and sheets showed quite similar activities here,[11] which could indicate a different reaction mechanism for the gold and copper catalysts. The deviations of the Raman and UV-vis results can be explained by the different penetration depths of the methods, with UV-vis spectroscopy being slightly more surface sensitive. Furthermore, our previous study[7] using $H_2{}^{18}O$ exchange experiments on Cu/CeO_2 during the WGS reaction have shown that lattice oxygen is more mobile for the sheets than for the polyhedra. Thus, lattice oxygen is transported from the bulk to the surface for the sheets, which is not the case for the polyhedra. The above aspects then lead to the increased absorption under reductive or reaction conditions for the polyhedra.

From the above discussion, we can conclude that the change of the reduction degree at the surface is not significant for the activity and that other aspects need to be taken into account, such as the mobility of lattice oxygen. In this context it should be mentioned that the sheets are generally much more reduced, which can be seen, for example, when comparing the F_{2g} position in the first reaction phase, which is 449.8 cm^{-1} for the sheets and 453.4 cm^{-1} for the polyhedra. Note that oxygen vacancies must be available for the reduction of CO_2, and since there are significantly fewer for polyhedra, the activity in the case of a redox mechanism is also lower. While there is no clear spectroscopic evidence to explain the steady decrease in activity for the polyhedra, it is possible that the copper species on the polyhedra change irreversibly under reaction conditions and that this is masked by the high absorption of the Ce^{4+}–Ce^{3+} charge transfers. Thus, in summary, the greater reducibility along with the greater activity of the sheets suggests a redox mechanism for the catalysts.

Next, we evaluate whether surface species such as carbonates, formates or hydroxides play a role in the reaction mechanism, which would be the case in an associative mechanism. For this purpose, we applied transient DRIFT spectroscopy, as described previously.[11] Here, the background was recorded in H_2, CO_2, or both, and then one of the gases was turned on or off. The advantage of these measurements is that only those species are detected which are really formed under reaction conditions, thus allowing differentiation between active and spectator species. As long as a signal is present for all measurements, *i.e.*, for all on and off experiments, the corresponding species is relevant for the reaction mechanism. Thereby it should be mentioned that a positive signal is caused by adsorption of possible reaction intermediates and a negative signal is caused by their desorption. Therefore, Fig. 3 shows the transient DRIFT spectra of the sheets (left) and the polyhedra (right) under the different conditions.

The transient spectra reveal that both sheets and polyhedra are characterized by bands in the carbonate, formate and hydroxide regions, as marked exemplarily for the sheets. In the carbonate range, there are also formate signals, but these are of low intensity and overlap with the carbonate signals. For this reason, we used the C–H vibrations to identify formates. Starting with the sheets, the left panel of Fig. 3 shows that switching CO_2 or H_2 on and off leads to essentially the same spectra, but with the opposite sign. Thus, we can conclude that these species are only formed under reaction conditions and are only stable if both reactants are present. With regard to carbon species, bidentate carbonates, bidentate formates and also polydentate carbonates are observed, based on the literature assignment.[4] The polydentate carbonates represent the smallest fraction but can be seen at 1367 cm^{-1}, especially in the case of the polyhedra. Apart from that, the spectra of the sheets and polyhedra show only small differences. In previous studies[4] the presence of polydentate carbonates was held responsible for the lower activity on higher-loaded catalysts (5 wt% Cu). In our case, however, they seem to be reversible, because the band at 1367 cm^{-1}, which is characteristic of polydentate carbonates, has both a positive and a negative sign with approximately the same intensity, showing that at least a small part of them may be involved in the reaction. Based on the transient spectra, bidentate carbonates, bidentate formates and hydroxides may play a role but in the carbonate region the intensities in the H_2 on or off experiments decrease significantly. While a background effect can be excluded, since in the CO_2 off experiment the

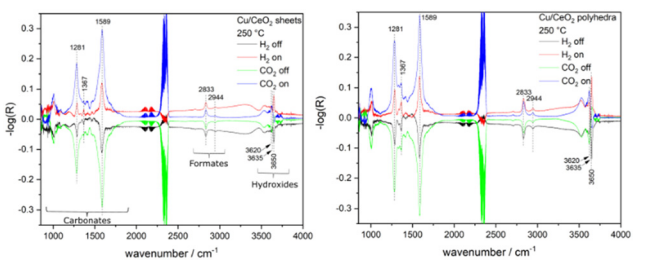

Fig. 3 Transient DRIFT spectra of Cu/CeO_2 sheets (left) and polyhedra (right). The spectra were recorded after pretreatment in H_2, CO_2 or H_2/CO_2 balanced in argon at 250 °C at a total gas flow of 100 ml min^{-1}. Prior to the measurements, the H_2 (CO_2) supply was switched on while CO_2 (H_2) remained constant or the H_2 (CO_2) was switched off while the CO_2 (H_2) remained constant. Shown are only the last spectra of a measurement series recorded after 12 min. For details see SI.†

background was also recorded under reaction atmosphere and here the intensity is significantly higher, the different intensities could be explained by the presence of gas-phase CO_2, leading to more carbonates on the surface, and to their desorption in the absence of CO_2. This behavior suggests that, in the presence of CO_2, a large fraction of surface carbonates act as spectators and are therefore not involved in the mechanism. When considering the C–H vibrations, such a decrease in intensity is not observed, thus suggesting their direct participation in the reaction mechanism.

Regarding the hydroxides, as in our previous study,[11] the bands at 3635 and 3650 cm^{-1} are most prominent and can be assigned to O–H stretching modes of bridged hydroxides, and, in particular, to an OH group on an oxidized surface and near a defect, respectively. These bands behave oppositely under reducing and oxidizing conditions, and thus respond only to the degree of surface reduction, making their participation in the reaction unlikely. However, the band at 3620 cm^{-1}, which can be assigned to triply bonded OH group (type III),[23] occurs in all spectra, so it might seem to be involved.

Finally, it should be mentioned that no Cu–CO IR bands are observed, which would be located red-shifted compared to the gas-phase CO signal. Thus, similar to the WGS reaction,[7] copper seems to have mainly an electronic effect on CeO_2, which significantly raises the activity in the rWGS reaction. This has already been described in earlier theoretical studies, where copper was shown to promote the formation of oxygen vacancies and the hydrogenation of CO_2.[24] Similarly, the Cu/CeO_2 catalysts behave fundamentally differently than the gold systems, in which hydrogen is activated by the noble metal *via* distinct hydrogen dissociation steps,[11] which are not observed for copper.

Conclusions

In summary, by applying *operando* spectroscopy to different low-loaded Cu/CeO_2 catalysts, the state of copper under reaction conditions can be probed, showing more cationic copper on the sheets and a dependence of the Cu^{2+} species on the gas phase. Furthermore, the sheets are significantly more reduced and have a higher mobility of lattice oxygen, whereby the larger changes in the degree of reduction (as indicated by the F_{2g} shift) correlate with the higher catalytic activity of the sheets. This behavior points to a redox mechanism. To investigate the involvement of adsorbates, transient DRIFTS measurements were performed, showing that bidentate formates are involved in the reaction, but due to their low intensity, the overall involvement of adsorbates is proposed to play a minor role. We conclude that the rWGS reaction over low-loaded Cu/CeO_2 catalysts proceeds simultaneously *via* both redox and associative mechanisms, but that the redox mechanism plays the predominant role. In this context, it is noticeable that corresponding Au/CeO_2 catalysts have shown an opposite mechanistic behavior,[11] which highlights the importance of the selection of the metal and its metal–support interaction. Our findings are expected to trigger mechanistic studies on supported catalysts for CO_2 activation, enabling the development of improved catalysts based on rational design. To this end, the above combination of *operando* and transient spectroscopic approaches has proven highly useful and is readily transferable to other oxide-supported catalysts.

We thank Henrik Hoyer for the synthesis of the catalysts and for preparatory experiments.

Conflicts of interest

There are no conflicts to declare.

Notes and references

1 F. Dong, Y. Meng, W. Han, H. Zhao and Z. Tang, *Sci. Rep.*, 2019, **9**, 12056.
2 A. Chen, X. Yu, Y. Zhou, S. Miao, Y. Li, S. Kuld, J. Sehested, J. Liu, T. Aoki, S. Hong, M. F. Camellone, S. Fabris, J. Ning, C. Jin, C. Yang, A. Nefedov, C. Wöll, Y. Wang and W. Shen, *Nat. Catal.*, 2019, **2**, 334–341.
3 G. Zhou, F. Xie, L. Deng, G. Zhang and H. Xie, *Int. J. Hydrogen Energy*, 2020, **45**, 11380–11393.
4 L. Lin, S. Yao, Z. Liu, F. Zhang, N. Li, D. Vovchok, A. Martínez-Arias, R. Castañeda, J. Lin, S. D. Senanayake, D. Su, D. Ma and J. A. Rodriguez, *J. Phys. Chem. C*, 2018, **122**, 12934–12943.
5 J. Zhu, Y. Su, J. Chai, V. Muravev, N. Kosinov and E. J. M. Hensen, *ACS Catal.*, 2020, **10**, 11532–11544.
6 P. Ebrahimi, A. Kumar and M. Khraisheh, *Catalysts*, 2022, **12**, 1101.
7 M. Ziemba, J. Weyel and C. Hess, *ACS Catal.*, 2022, **12**, 9503–9514.
8 M. Ziemba, C. Schilling, M. V. Ganduglia-Pirovano and C. Hess, *Acc. Chem. Res.*, 2021, **54**, 2884–2893.
9 H.-X. Liu, S.-Q. Li, W.-W. Wang, W.-Z. Yu, W.-J. Zhang, C. Ma and C.-J. Jia, *Nat. Commun.*, 2022, **13**, 867.
10 Y. Chen, J. Lin and X. Wang, *Chem. Commun.*, 2022, **58**, 208–222.
11 M. Ziemba, J. Weyel and C. Hess, *Appl. Catal., B*, 2022, **301**, 120825.
12 A. Li, D. Yao, Y. Yang, W. Yang, Z. Li, J. Lv, S. Huang, Y. Wang and X. Ma, *ACS Catal.*, 2022, **12**, 1315–1325.
13 C. W. M. Castleton, J. Kullgren and K. Hermansson, *J. Chem. Phys.*, 2007, **127**, 244704.
14 M. Zabilskiy, P. Djinović, E. Tchernychova, O. P. Tkachenko, L. M. Kustov and A. Pintar, *ACS Catal.*, 2015, **5**, 5357–5365.
15 H. Praliaud, *Appl. Catal., B*, 1998, **16**, 359–374.
16 A. N. Pestryakov, V. P. Petranovskii, A. Kryazhov, O. Ozhereliev, N. Pfänder and A. Knop-Gericke, *Chem. Phys. Lett.*, 2004, **385**, 173–176.
17 G. H. Chan, J. Zhao, E. M. Hicks, G. C. Schatz and R. P. van Duyne, *Nano Lett.*, 2007, **7**, 1947–1952.

18 Y. Bu, J. W. H. Niemantsverdriet and H. O. A. Fredriksson, *ACS Catal.*, 2016, **6**, 2867–2876.
19 J. Chen, Y. Zhan, J. Zhu, C. Chen, X. Lin and Q. Zheng, *Appl. Catal., A*, 2010, **377**, 121–127.
20 M. Zabilskiy, P. Djinović, B. Erjavec, G. Dražić and A. Pintar, *Appl. Catal., B*, 2015, **163**, 113–122.
21 M. Ziemba, M. V. Ganduglia-Pirovano and C. Hess, *Faraday Discuss.*, 2021, **229**, 232–250.
22 Y. Lee, G. He, A. J. Akey, R. Si, M. Flytzani-Stephanopoulos and I. P. Herman, *J. Am. Chem. Soc.*, 2011, **133**, 12952–12955.
23 A. Laachir, V. Perrichon, A. Badri, J. Lamotte, E. Catherine, J. C. Lavalley, J. el Fallah, L. Hilaire, F. le Normand, E. Quéméré, G. N. Sauvion and O. Touret, *J. Chem. Soc., Faraday Trans.*, 1991, **87**, 1601–1609.
24 Z.-Q. Wang, H.-H. Liu, X.-P. Wu, P. Hu and X.-Q. Gong, *Catalysts*, 2022, **12**, 963.

